How Do Fatty Acids Cause Allosteric Binding of Drugs to Human Serum Albumin?

Victor Tuan Giam Chuang[1] and Masaki Otagiri[1,2]

Received July 25, 2002; accepted July 29, 2002

Purpose. This study was undertaken to investigate how fatty acids cause the allosteric binding of drugs to human serum albumin (HSA). The influence of fatty acids on the binding of ketoprofen (KP), an NSAID, to HSA was examined by using a photoaffinity labeling technique.

Methods. Ultrafiltration was performed to quantitate the concentration of free KP. HSA, photolabeled with KP in the presence of myristate (MYR), octanoate, and diazepam, was cleaved with cyanogen bromide, separated by Tricine sodium dodecyl sulfate polyacrylamide gel electrophoresis and subsequently analyzed by autoradiography.

Results. The addition of MYR at molar ratios from 4 to 5, but not from 1 to 2, causes substantial increases in unbound KP for KP:HSA ratios of 0.5 and 1. The addition of two or more moles of MYR, octanoate, and diazepam per mole of HSA caused a pronounced decrease in the labeling of the 11.6- and 13.5-kDa peptides. However, only MYR showed an increase in labeling of the 20 kDa and, especially, the 9.4-kDa peptides. At MYR:HSA ratios in excess of 3, a decrease in the extent of labeling of the 9.4-kDa peptide was observed.

Conclusion. Long-chain fatty acids regulate the binding properties of HSA in a complex manner, in which a simultaneous competitive and allosteric mechanism operates and which mainly involves domain I.

KEY WORDS: human serum albumin; ketoprofen; fatty acid; photoaffinity labeling; allosteric binding; chain length.

INTRODUCTION

In addition to its important role in stabilizing the physical environment of the blood, human serum albumin (HSA) is well known as a major transport and depot protein for long-chain fatty acid anions (1). Because of its extraordinary binding capacity, HSA is also capable of binding a wide range of drugs (2). In different types of studies, especially competition experiments, Sudlow reported on the presence of two primary drug-binding sites on the protein, referred to as sites I, also called the warfarin-binding site, and site II, also called the indole- and benzodiazepine-binding site. Crystallographic studies have shown that the protein is composed of three structurally homologous domains (I–III), which form a heart-shaped tertiary structure. Each domain has two subdomains (A and B), the main structures of which are six (A) and four (B) α-helices. Drug-binding sites I and II of HSA are located in subdomains IIA and IIIA, respectively (3).

Because plasma typically contains fatty acids, their presence is important in investigations of all physiologically related albumin-binding interactions. It has been reported that fatty acids bind to at least five different sites with high or relatively high affinity and that this binding is distributed unequally among the three domains (4). Because two of these high-affinity binding sites are located in subdomain IIIA, which is also the location of a major drug-binding site, the displacement of a bound drug by fatty acids would be expected to occur in this region of the protein. However, because HSA carries, on average, only two molecules of fatty acid under normal physiological conditions, and because the relative affinity of these five high-affinity binding sites is currently unknown, the significance of such drug displacement interactions remains to be elucidated.

In addition, numerous subsequent studies have shown that the presence of fatty acids has unpredictable effects on drug binding, and both cooperative and competitive interactions have been observed. In most cases, the mechanism of interaction of these ligands with HSA and the relative importance of the different domains and subdomains of HSA for ligand binding remain incompletely clarified. Therefore, the existence of the sites does not, in itself, provide a complete explanation for the unique and complex ligand-binding properties of HSA.

Ketoprofen (KP) is an arylpropionic acid that binds with high affinity to Sudlow's site II in subdomain IIIA. Because it has a benzophenone moiety, it can be used directly as a photolabeling reagent that is highly regioselective (5). Because HSA contains six methionine residues, with the simultaneous reduction of the 17 disulfide bonds and modification of the thiol groups, treatment with cyanogens bromide (CNBr) would be expected to produce seven fragments with theoretical molecular weights of 20, 13.5, 11.6, 9.4, 4.1, 4.0, and 3.5 kDa, which can be identified by their mobilities on sodium dodecyl sulfate (SDS) containing gels (Fig. 1). The amino acid sequence of the fragment, which corresponds to the theoretical molecular weight, had also been determined in several previous studies (6,7). The mapping of these seven fragments within the structural locations and their electrophoresis characteristics showed that the fragments can be used as a rough representation of the three domains, thus allowing any change in the photolabeling pattern of the subdomains to be monitored (5).

In this study, HSA was photolabeled with [^{14}C]KP in the absence and presence of myristate (MYR) and octanoate (OCT), and another aromatic drug, diazepam (DZP). On the basis of results obtained, the significance of drug displacement by fatty acids was examined by an attempt to devise a map of relative affinity of the five binding sites of fatty acids. Based on this map, a possible mechanism of the interplay between fatty acids and therapeutic agent in HSA binding is proposed.

MATERIALS AND METHODS

Materials

HSA was donated by the Chemo-Sera-Therapeutic Research Institute (Kumamoto, Japan). HSA was defatted with

[1] Faculty of Pharmaceutical Sciences, Kumamoto University, 5-1 Oe-honmachi, Kumamoto 862-0973, Japan.

[2] To whom correspondence should be addressed. Biopharmaceutics Laboratory, Faculty of Pharmaceutical Sciences, Kumamoto University, 5-1 Oe-honmachi, Kumamoto 862-0973, Japan. (e-mail: otagirim@gpo.kumamoto-u.ac.jp)

ABBREVIATIONS: HSA, human serum albumin; KP, ketoprofen; MYR, myristate; OCT, octanoate; DZP, diazepam; CNBr, cyanogen bromide.

0724-8741/02/1000-1458/0 © 2002 Plenum Publishing Corporation

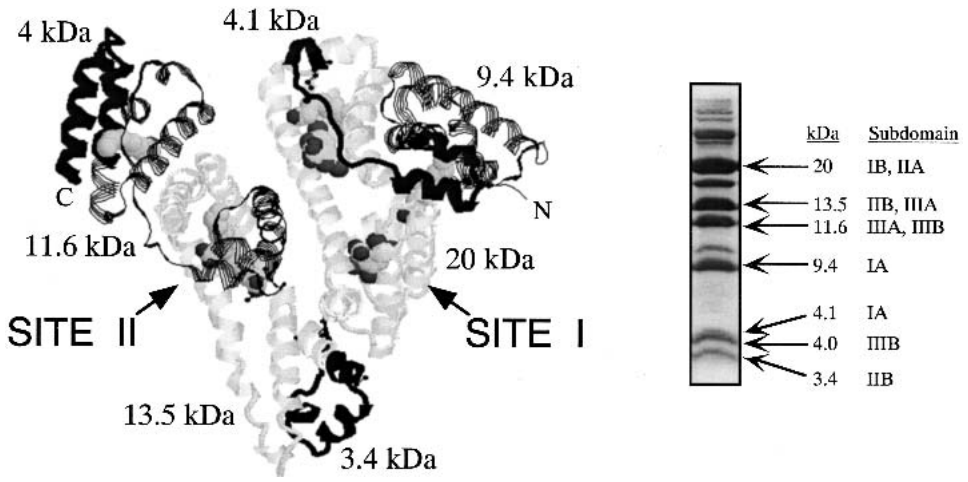

Fig. 1. Right: Tricine SDS-PAGE of reduced and pyridylethylated HSA cleaved with cyanogen bromide. Left: Crystal structure of HSA complexed with myristate and triiodobenzoate, with the position of the seven CNBr fragments as well as their molecular weights indicated. The figure was prepared by using RasMol v2.6 software as taken from PDB ID 1bke. The six methionine residues and their positions in HSA are shown in black. N and C represent N-terminus and C-terminus, respectively. Parallel strand: 9.4- and 11.6-kDa peptides; solid ribbon in gray: 20- and 13.5-kDa peptides; solid ribbon in black: 4.1, 3.4, 4.0-kDa peptides. The locations of the two primary drug-binding sites, site I and site II, are also shown.

an aqueous suspension of activated charcoal at 0°C, acidified with H_2SO_4 to pH 3, dialyzed exhaustively against deionized water, and then lyophilized. The HSA used in this study showed only one band, corresponding to approximately 66 kDa in SDS-polyacrylamide gel electrophoresis (PAGE). Racemic [^{14}C]KP (96% pure) with a specific radioactivity of 12.95 μCi/mg was obtained from Hisamitsu Pharmaceutical Co., Inc., Tosu Laboratories (Saga, Japan). Myristic acid sodium salt (MYR) was obtained from Tokyo Kasei Kogyo Co., Ltd., Japan. Sodium caprylate (OCT) was obtained from Wako Pure Chemical Industries, Ltd., Japan. Diazepam (DZP), Lot No. N-243 was obtained from Sumitomo Pharmaceuticals (Osaka, Japan). Cyanogen bromide (CNBr) was obtained from Nacalai Tesque Inc., (Kyoto, Japan). All other chemicals were of analytical grade.

Ligand Binding

Ultrafiltration was performed by using Centrifree MPS-1 (Amicon Division, Danvers, MA, USA). Ligands were added to 1 mL of HSA (40 μM) in 20 mM Tris buffer, at pH 7.4, and preincubated at 25°C for 30 min before centrifugation (2000 rpm for 40 min). A 200-μL aliquot was added to a scintillation cocktail in a scintillation vial (Pyrex), vortexed, and counted by using a Scintillation Counter (Beckman). No adsorption of the ligands to membrane or apparatus was detectable.

Photoaffinity Labeling

HSA (40 μM) was incubated with [^{14}C]KP (20 μM), in the absence of and the presence of different concentrations of MYR, OCT, and DZP, in 100 μL of 20 mM Tris buffer, at pH 7.4, in a 1.5-mL Eppendorf tube at room temperature in the dark for 60 min. The incubation mixture was then placed on ice and irradiated for 30 min at a wavelength of >320 nm by a 100-W black light/blue lamp (Ultra-Violet Products, Inc., San Gabriel, CA, USA) at a distance of 10 cm. After irradiation, the photolabeled HSA was precipitated by adding 1 mL of acetone, followed by centrifugation at 14,000 rpm for 10 min. The pellet was washed with 1 mL of ethanol and centrifuged a second time before reductive pyridylethylation was performed.

Reductive Pyridylethylation

One hundred microliters of the reduction medium (6 M Guanidium HCl, 20 mM Tris buffer, pH 8.0, 20 mM EDTA and 20 mM DTT) was added to the pellet, which was then incubated under N_2 at 37°C for at least 12 h. After the addition of 1 μL of 4-vinylpyridine, the mixture was incubated under N_2 for an additional hour at room temperature in the dark. At the end of the pyridylethylation reaction, 1 mL of acetone was added to the mixture to terminate the reaction. The suspension was then vortexed vigorously followed by a light centrifugation. One hundred microliters of milli-Q water was added, the mixture was further vortexed, and the pyridylethylated HSA was precipitated after standing on ice for 1 h to remove the salts and unreacted 4-vinylpyridine, the suspension was centrifuged at 14,000 rpm for 10 min. Finally, the pellet was washed with 1 mL of ethanol before CNBr cleavage.

CNBr Cleavage and Tricine SDS-PAGE

The pyridylethylated pellet was dissolved in 100 μL of 0.64 mg CNBr in 70% formic acid (CNBr:Methionine residues = 200:1) and incubated under N_2 for 24 h in the dark at room temperature. One millimeter of milli-Q water was added at the end of the CNBr cleavage to stop the reaction, and the resulting mixture was lyophilized. The lyophilized CNBr fragments were resuspended in 100 μL of 0.1% TFA, and the protein concentration was determined by a Bradford assay. Fifteen micrograms of the fragment mixture was applied to each lane of the gel and separated with tricine SDS-PAGE.

Autoradiographic Analysis

After electrophoresis, the gel was stained with Coomassie Brilliant Blue R250 and completely dried with a

vacuum heater. The dried gel was then placed in contact with an imaging plate (BAS III, Fuji Photo Film Co.) in a cassette (BAS cassette 2040) at room temperature for 48 h. The imaging plate was scanned by using a Bio-Imaging Analyzer, FLA-3000 model (Fuji Photo Film Co.) and analyzed by using the Fuji Film Science Lab 98 software, L Process V1.6 and Image Gauge V3.1 (Fuji Film).

Statistical Analysis

All data are presented as means ± SD. Statistical analysis using the paired Student's *t* test was performed on the data where appropriate. The degree of significance for a two-tailed test, p, is given.

RESULTS

Binding of KP in the Presence and Absence of MYR

As can be seen from Table I, the addition of MYR at molar ratios of from 4 to 5, but not from 1 to 2, causes substantial increases in unbound KP for KP:HSA ratios of 0.5 and 1 ($n = 4$, $p < 0.001$). At a molar ratio of 3, MYR appears to have an intermediate effect with respect to KP displacement. This phenomena was confirmed by repeating the experiment at KP:HSA ratios of between 0.5 and 1 (data not shown).

Photolabeling of HSA with [^{14}C]KP at a Constant [^{14}C]KP:HSA Ratio of 1:2, in the Presence and Absence of Different Molar Ratios of MYR

To focus on the high-affinity binding site for KP, photolabeling was first performed at a drug to protein molar ratio of 1:2. In the absence of MYR, the incorporation of KP into the 11.6- and 13.5-kDa fragments, which contain portions of subdomain IIIA, was favored, with minor binding to the fragments having molecular weights of 9.4 and 20 kDa (Fig. 2).

Irradiation of the KP-HSA complex with increasing concentrations of MYR at molar ratios from 1 to 3 caused KP displacement from the 11.6-kDa fragment resulting in a decreased level of labeling of the fragment. In particular, a MYR:HSA ratio of 2 results in a significant displacement of KP from the 11.6-kDa fragment. This finding indicates that the second molecule of MYR binds competitively to the primary binding site of KP (Table II), because no displacement was found for the other 13.5- and 20-kDa fragments except a concomitant and extensive increase in the labeling of the 9.4-kDa fragment. The displaced KP was found to have rebound mainly to the 9.4-kDa fragment and did so to a larger extent than would be expected. In principle, the same observation was made for the 20-kDa fragment but to a minor extent.

The allosteric effects of MYR on KP binding reached a maximum at a MYR:HSA ratio of 3 (Fig. 2). The larger than

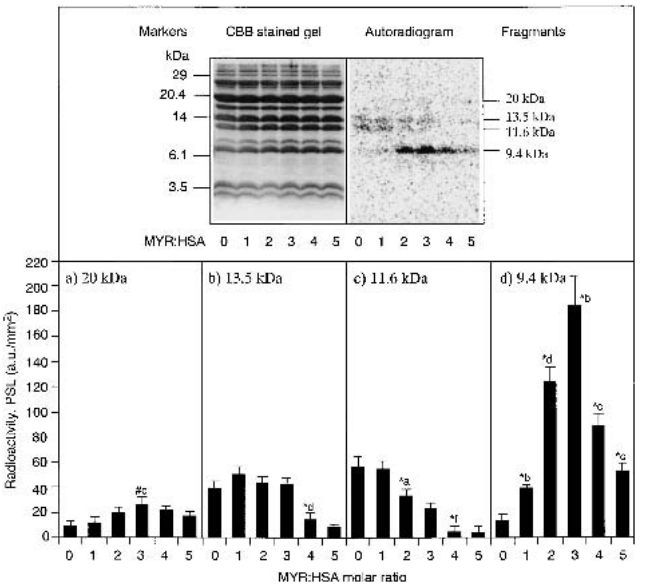

Fig. 2. CNBr fragments of HSA after [^{14}C]KP photoaffinity labeling in the presence of different MYR concentrations. Upper panel: Left side shows a Coomassie Brilliant Blue-stained gel, whereas the right side represents an autoradiogram of the gel. The incubation ratio for [^{14}C]KP:HSA was 1:2. Lower panel: Incorporation of radioactivity into four CNBr fragments at different MYR concentrations. Each bar represents means ± SD from three replicates. #, when compared with MYR:HSA = 0; *, when compared with the previous MYR:HSA ratio. a, $p < 0.05$; b, $p < 0.02$; c, $p < 0.01$; d, $p < 0.005$; e, $p < 0.002$; f, $p < 0.001$.

Table I. Free Concentrations (μM) of [^{14}C]KP, as Determined by Ultrafiltration

	Free KP concentration (μM)	
	KP:HSA = 0.5	KP:HSA = 1
Myr:HSA = 0	1.31 ± 0.04	2.85 ± 0.07
Myr:HSA = 1	1.24 ± 0.04	2.69 ± 0.07
Myr:HSA = 2	1.46 ± 0.04	3.13 ± 0.08
Myr:HSA = 3	1.62 ± 0.04	3.87 ± 0.10
Myr:HSA = 4	2.01 ± 0.05*	4.30 ± 0.10*
Myr:HSA = 5	2.06 ± 0.05*	4.32 ± 0.10*

Note: The binding of KP (20, 40 μM) to HSA (40 μM) in the absence and presence of different molar ratios of MYR. Free KP concentration is represented by the means ± SD from four replicates. The free concentrations of KP at various MYR:HSA ratios were compared with that of MYR:HSA = 0 by using paired Student's *t* test.
* $p < 0.001$.

Table II. Assignment of Ligand-Binding Sites to HSA

Subdomain	KP[a]	MYR[b]	OCT[a]	DZP[a]
I A	2[c]	5[e]		2
I B	3[d]	3		
II A (Sudlow's site I)				
II B				
III A (Sudlow's site II)	1	2[f], 4[g]	1	1
III B		1[h]		

[a] 1 and 2 represent the high-affinity-binding site and a secondary site, respectively.
[b] 1–5 represent successive binding sites with decreasing binding affinity.
[c] Affinity is increased allosterically by the presence of MYR.
[d] Induced by the presence of MYR.
[e] Subdomain IIA also takes part in forming this binding site.
[f] MYR-molecule number 2 binds to the same region as the first molecule of KP, OCT, and DZP.
[g] Subdomain IIB also takes part in forming this binding site.
[h] References 1,3, 13–15.

expected rebinding of KP to the two latter fragments is probably the reason why no significant effect of MYR on KP binding was found in the ultrafiltration experiment. At MYR:HSA ratios > 3, the displacement of KP was observed for all fragments. In the 11.6-kDa fragment, KP covalent binding was nearly completely blocked, a finding that supports the proposal that MYR binds with a high affinity to the primary KP-binding site.

Photolabeling of HSA with [^{14}C]KP at a Constant [^{14}C]KP:HSA Ratio of 2:1, in the Presence and Absence of Different Molar Ratios of MYR

The effect of MYR was also studied at a higher KP to HSA molar ratio (2:1 instead of 1:2). This was done to saturate the high-affinity KP site, and hence, to achieve a more frequent interaction of KP to the secondary sites. This was observed as an increase in labeling of the 13.5-, 11.6-, and 9.4-kDa peptides. As is apparent from Fig. 3, essentially the same displacement and allosteric binding effects were observed. However, the displacing effect of MYR on primary KP binding is more clearly seen, as is the allosterically increased binding to the 20-kDa fragment.

Photolabeling of HSA with [^{14}C]KP in the Presence and Absence of Different Molar Ratios of OCT

The effect of the shorter-chained fatty acid OCT on the KP labeling of HSA at a 1:2 molar ratio is illustrated in Fig. 4. The effects of OCT differ from those of MYR, especially with respect to the three smaller fragments. For both the 13.5- and the 11.6-kDa fragments, a nearly uniform decrease in radioactive labeling was observed with increasing OCT concentrations. Even though the high-affinity constant for OCT is lower than that of MYR [5], the addition of the former at an OCT:HSA ratio of 1 caused a pronounced decrease in the photolabeling of the 11.6- and 13.5-kDa fragments, indicating that OCT and KP share a common primary binding site (Table II). Higher concentrations of OCT caused further decreases in the labeling of the two fragments by KP. However, in contrast to MYR, no significant effects on the binding of KP to the 9.4- and 20-kDa fragments were detected. These fragments were able to bind OCT with a secondary affinity, but the binding constant for such sites is so much lower [$K_2 = 3 \times 10^2\ M^{-1}$ (8)] than that for KP [$K_2 = 4 \times 10^5\ M^{-1}$ (9)] that a significant displacement effect would not be expected. On the other hand, it is noteworthy that OCT, in contrast to MYR, did not cause an increase in KP incorporation into the fragments. This finding suggests that OCT, which has a shorter chain length and lower binding affinity, is unable to induce significant allosteric effects in subdomains IA and IB.

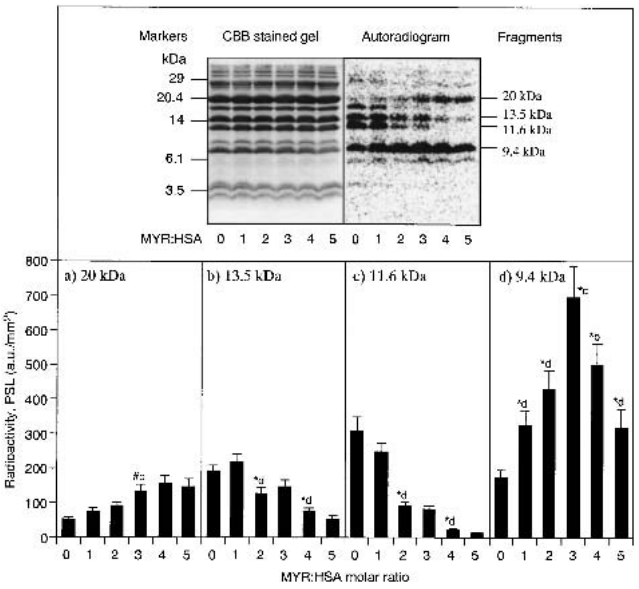

Fig. 3. CNBr fragments of HSA after [^{14}C]KP photoaffinity labeling in the presence of different MYR concentrations. Upper panel: Left side shows a Coomassie Brilliant Blue-stained gel, whereas the right side represents an autoradiogram of the gel. The additional bands seen in the autoradiogram most probably represent incompletely cleaved fragments. In this case, the incubation ratio for [^{14}C]KP:HSA was 2:1. Lower panel: Incorporation of radioactivity into four CNBr fragments at different MYR concentrations. Each bar represents means ± SD from three replicates. #, when compared with MYR:HSA = 0; *, when compared with the previous MYR:HSA ratio. a, $p < 0.05$; b, $p < 0.02$; c, $p < 0.01$; d, $p < 0.005$; e, $p < 0.002$; f, $p < 0.001$.

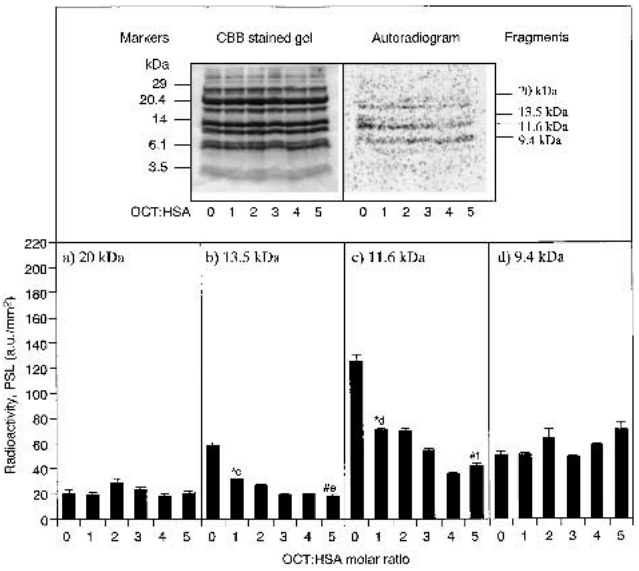

Fig. 4. CNBr fragments of HSA after [^{14}C]KP photoaffinity labeling in the presence of different OCT concentrations. Upper panel: Left side shows a Coomassie Brilliant Blue-stained gel, whereas the right side represents an autoradiogram of the gel. The incubation ratio for [^{14}C]KP:HSA was 1:2. Lower panel: Incorporation of radioactivity into four CNBr fragments at different OCT concentrations. Each bar represents mean ± SD from three replicates. #, when compared with OCT:HSA = 0; *, when compared with the previous OCT:HSA ratio. a, $p < 0.05$; b, $p < 0.02$; c, $p < 0.01$; d, $p < 0.005$; e, $p < 0.002$; f, $p < 0.001$.

Photolabeling of HSA with [^{14}C]KP in the Presence and Absence of Different Molar Ratios of DZP

The effect of another added aromatic ligand, namely DZP, on photolabeling is illustrated in Fig. 5. The sequential addition of increasing concentrations of DZP caused parallel decreases in the levels of radioactivity of the 13.5- and 11.6-kDa fragments. A displacing effect would be expected, because DZP has also been reported to bind to subdomain IIIA with a high affinity (8,10). However, the displacement pattern

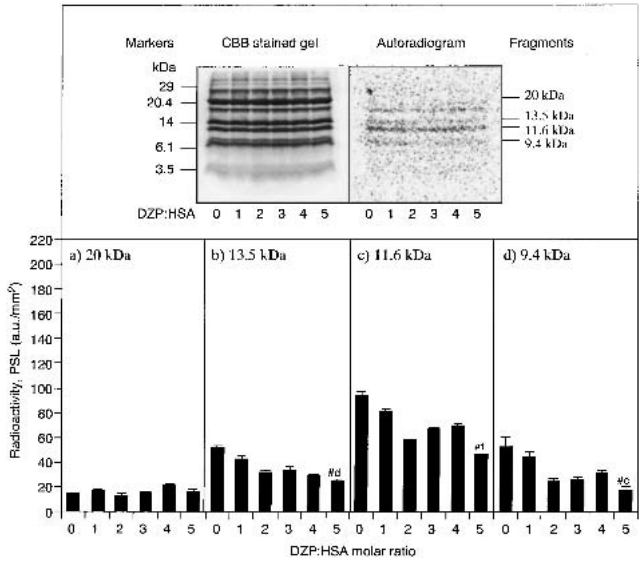

Fig. 5. CNBr fragments of HSA after [^{14}C]KP photoaffinity labeling in the presence of different concentrations of DZP. Upper panel: Left side shows a Coomassie Brilliant Blue-stained gel, whereas the right side represents an autoradiogram of the gel. The incubation ratio for [^{14}C]KP:HSA was 1:2. Lower panel: Incorporation of radioactivity into four CNBr fragments at different DZP concentrations. Each bar represents means ± SD from three replicates. #, when compared with DZP:HSA = 0; *, when compared with the previous DZP:HSA ratio. a, $p < 0.05$; b, $p < 0.02$; c, $p < 0.01$; d, $p < 0.005$; e, $p < 0.002$; f, $p < 0.001$.

is different from that of OCT. These patterns could be caused by differences in binding constants [DZP: $K_1 = 3.8 \times 10^5\ M^{-1}$; OCT: $K_1 = 1.6 \times 10^6\ M^{-1}$ (8)] and/or differences in the detailed construction of the two binding sites. DZP also caused a parallel decrease in the degree of KP photolabeling to the 9.4-kDa fragment, which contains subdomain IA, indicating the presence of a secondary DZP-binding site and the absence of allosteric effects in this fragment (Table II). The assignment of such a site to subdomain IA is in agreement with the results of Dockal *et al.* (11), who examined the binding of ligands to the recombinant domains of HSA. In contrast to the other fragments, no apparent changes in the photolabeling pattern could be observed for the 20-kDa fragment. Thus, neither DZP nor OCT is able to increase KP binding through allosteric effects.

DISCUSSION

Relative Binding Site Affinity of the Fatty Acid

The locations of five fatty acid-binding sites with apparent electrostatic features on HSA were recently reported, but it was not possible to decipher the relative affinity among these sites. One possibility for shedding light on the above problem would be to covalently link fatty acids to HSA and then dissect the protein. However, fatty acids cannot themselves be used as labeling agents, because the chemical modification of fatty acids can result in covalent binding to occur outside the actual sites for reversible binding. Because MYR binds HSA at higher affinities than KP (9,12), MYR would be able to compete and displace KP from the binding sites. In a previous study, we showed that KP primarily photolabeled subdomain IIIA, with a minor amount of labeling to subdomain IA, which is consistent with other experimental results indicating that KP binds primarily to subdomain IIIA (5). Therefore, in the present study we used [^{14}C]KP as a photoaffinity-labeling agent to label HSA in the presence of different concentrations of MYR for purposes of examining the photolabeling pattern of KP and hence the significance of the displacement by MYR, because this method converts the rapid equilibrium kinetics to irreversible covalent bonds, permitting more conventional biochemical approaches to be used to identify the binding sites.

It has been reported that three high affinity-binding sites for laurate are located at subdomains IB, IIIA, and IIIB (3). Based on convincing biochemical evidence, the long-chain fatty acid-binding site with the highest affinity is located at subdomain IIIB, thus the highest affinity-binding site for MYR can be assigned to that located at subdomain IIIB (1,3,13–15). This assignment is consistent with the photoinhibition results in which no apparent decrease in labeling for all four peptides could be observed at a MYR:HSA ratio of 1 (Figs. 2 and 3). Because the extent of decrease in labeling is the largest for the 11.6-kDa peptide at a MYR:HSA ratio of 2, the second high-affinity site can, therefore, be assigned to the site that exists in subdomain IIIA.

Up to a MYR:HSA ratio of 3, an increase in labeling was observed for both the 20- and 9.4-kDa peptides. A crystallographic study has shown that MYR binding at subdomain IB coexist with another ligand, namely, triiodobenzoate (4) (Fig. 1). Assuming that KP will also cobind with MYR at this region, although it may not bind in a manner similar to triiodobenzoate, subdomain IB houses the third high-affinity site because subdomain IB is contained in the 20-kDa peptide.

A significant decrease in labeling was observed for the 13.5- and 9.4-kDa peptides at a MYR:HSA ratio of 4, but only the 9.4-kDa showed a further decrease in labeling at a MYR:HSA ratio of 5. In the crystallographic study, cooperative binding between fatty acids was observed for subdomain IIIA where the first molecule of MYR that binds to this region facilitates the binding of a subsequent molecule of MYR (Fig. 6). The fourth site is, most likely, located at the interface of subdomains IIB and IIIA, because of the fact that one of the two binding sites that belongs to the highest affinity sites would have been occupied by the first three molecules of MYR. This ultimately leaves the binding region at the interface of subdomains IA and IIA as the fifth site.

Although assigning the relative affinities to the five strongest MYR-binding sites based on the photolabeling displacement pattern is an indirect method and will require further confirmation (Fig. 6), interpretation of the present data, together with the recently available MYR-HSA complex crystallographic data, should be able to provide a preliminary starting point for future investigations.

Allosteric Binding Effect Induced by Long-Chain Fatty Acids

Other studies have shown that the addition of up to three moles of long-chain fatty acids enhances the binding of ligands, such as warfarin, which bind primarily to site I in subdomain IIA (16–18). This increase in binding is usually explained by a cooperative effect exerted on site I by fatty acids, which are strongly bound to domain III. However, because an increase in labeling of the 20- and 9.4-kDa peptides was not

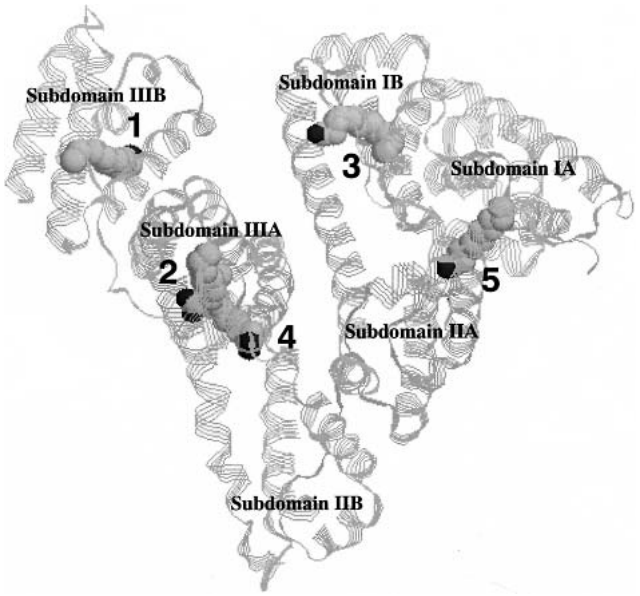

Fig. 6. Crystal structure of HSA liganded with MYR. The figure is shown in parallel strands (PDB ID, 1bj5).

observed for fatty acids with a shorter methylene chain length, namely, OCT (Fig. 4), and an aromatic ligand DZP (Fig. 5), which bind primarily to subdomain IIIA, binding to this region is less likely to generate the allosteric binding effect. On the other hand, in a crystallographic study of the HSA-MYR-warfarin complex, Petitpas *et al.* proposed that the presence of MYR at the interface of subdomain IA could be the reason for the increased binding affinity of warfarin in the presence of fatty acids (19). However, in the crystallographic study, six molecules of MYR, including that in subdomain IA, were found to coexist with warfarin. On the other hand, in conventional binding experiments, a decrease in the binding affinity of warfarin had been observed when more than three moles of fatty acid are bound per mole of HSA (2). Therefore, the influence of MYR bound at the interface of subdomain IA in enhancing warfarin-binding affinity to HSA needs further justification.

In the ultrafiltration experiment, the presence of MYR at a MYR:HSA ratio of 2 did not significantly increase the free concentration of KP as shown in Table I. The displacing effects of fatty acids can only be observed at MYR:HSA ratios higher than 3. On the other hand, in the photolabeling experiment, MYR but neither OCT nor the aromatic ligand DZP was able to increase KP binding to the 20-kDa fragment (subdomains IB and IIA) and, especially, to the 9.4-kDa fragment (subdomain IA). The increase in labeling for these two peptides reached a maximum at a MYR:HSA ratio of 3. Simultaneously, a decrease in labeling for the 11.6-kDa and 13.5-kDa peptides (subdomains IIIA and IIIB) was observed for all MYR concentrations. Of course, it is difficult to quantitatively link the results of both experiments because they are of different nature. However, photolabeling techniques allow the reversible binding regions of the protein to be examined through the formation of a covalent bond between the ligand and the binding site. Hence, changes in the KP-binding region on HSA can be monitored in the presence of different MYR concentrations.

Based on the results herein, a reasonable explanation for the phenomena can be proposed. Namely, that the addition of two or more moles of MYR per mole of HSA causes a pronounced displacement of KP, but this effect does not necessarily mean that the concentration of unbound KP increases to any extent, because MYR allosterically increases the binding of KP to domain I.

The increase in labeling of the 20-kDa peptide, which contains subdomain IB, in the presence of MYR can be explained by the binding facilitating effect of MYR where a ligand binds to this region only in the presence of MYR. Such a phenomenon has been observed for the simultaneous binding of MYR and triiodobenzoate (4) and probably for the simultaneous binding of MYR and warfarin (19) as well. On the other hand, the increased labeling effect observed for MYR:HSA ratios of 1–3 in the 9.4-kDa peptide must have been induced by the first three MYR molecules. A decrease in labeling could be observed for the 9.4-kDa peptide (subdomain IA) starting from a MYR:HSA ratio of 4, indicating a displacing effect by MYR in this region.

Because there is reason to believe that the third strongest MYR-binding site is located in subdomain IB (Table II), and because the maximal cooperative effect on KP binding was observed for a MYR:HSA ratio of 3 (Figs. 2 and 3), conformational changes in subdomain IB could involve subdomain IA, thus improving the affinity of the KP site placed here and/or create new sites for drug binding. An interesting finding in this regard is that palmitate and stearate, but not OCT, was reported to inhibit the modification of His146, which is located in subdomain IB by *N*-dansylaziridine (20). The fact that OCT did not show such an increased labeling effect involving the 9.4-kDa peptide suggests that the chain length of the fatty acid (number of methylene groups) must have played a role in the induction of this binding, because fatty acids of different chain lengths (10–18 C-atoms) were shown in a crystallographic studies to adopt a binding orientation similar to subdomain IB regardless of their chain length (21).

In the crystallographic analyses by Bhattacharya *et al.* (21), they reported that OCT could not be cocrystallized with HSA in a form that is isomorphous with HSA, when complexed with fatty acids of longer chain lengths. This may be due to the fact that the methylene tail of OCT is too short to make stabilizing contacts with subdomain IA. Therefore, MYR (and fatty acids with longer chain lengths), in contrast to OCT, has a sufficient chain length to permit its interaction with His146 and inhibits its interaction with *N*-dansylaziridine. In addition to this effect, MYR also is more strongly hydrophobic than OCT; these factors could explain, in part, why only the longer chained fatty acids are able to induce the allosteric binding of KP to subdomain IA. Because the tip of the methylene tail of a fatty acid with a sufficient chain length was shown to be able to interact with His146 (20,21), the MYR-induced allosteric binding effect involving subdomain IA could have occurred through interactions with this residue.

CONCLUSION

Using photoaffinity-labeling techniques, we have shown in the present study that long-chain fatty acids are able to regulate the binding properties of HSA in a complex manner, involving both competitive and allosteric mechanisms and that this regulation depends on the methylene chain length of

the fatty acid. In contrast, it is likely that medium-chain fatty acids result in significant drug displacement interactions at concentrations lower than that of their long-chain counterparts, because medium-chain fatty acids are less capable of allosterically increasing the rebinding of the displaced ligand to domain I. Under normal physiologic conditions, HSA carries ~0.1–2 mol of fatty acid per mol of protein. Therefore, unless there is an otherwise persistent increase in plasma fatty acid levels (22), drug displacement through protein-binding interactions by long-chain fatty acid would be expected to play a minimum role if any. In contrast to MYR, the medium-chain fatty acid OCT binds with a high affinity to site II and therefore competes directly with, for example, KP, DZP, and L-tryptophan for a primary binding site (8,23). The displacement of other site II ligands by medium-chain fatty acids most likely results in significant increases in the free concentration of the displacees (24), because medium-chain fatty acids are not capable of allosterically increasing the binding of these to domain I.

REFERENCES

1. T. Peters, Jr. *All about albumin: Biochemistry, genetics, and medical applications,* Academic Press, San Diego, California, 1996.
2. U. Kragh-Hansen. Molecular aspects of ligand binding to serum albumin. *Pharmacol. Rev.* **33**:17–53 (1981).
3. D. C. Carter and J. X. Ho. Structure of serum albumin. *Adv. Protein Chem.* **45**:153–203 (1994).
4. S. Curry, H. Mandelkow, P. Brick, and N. Franks. Crystal structure of human serum albumin complexed with fatty acid reveals an asymmetric distribution of binding sites. *Nat. Struct. Biol.* **5**: 827–835 (1998).
5. V. T. G. Chuang, A. Kuniyasu, H. Nakayama, Y. Matsushita, S. Hirono, and M. Otagiri. Helix 6 of subdomain III A of human serum albumin is the region primarily photolabeled by ketoprofen, an arylpropionic acid NSAID containing a benzophenone moiety. *Biochim. Biophys. Acta* **1434**:18–30 (1999).
6. R. G. Eckenhoff. Amino acid resolution of halothane binding sites in serum albumin. *J. Biol. Chem.* **271**:15521–15526 (1996).
7. R. G. Eckenhoff, C. E. Petersen, C. E. Ha, and N. V. Bhagavan. Inhaled anesthetic binding sites in human serum albumin. *J. Biol. Chem.* **275**:30439–30444 (2000).
8. U. Kragh-Hansen. Octanoate binding to the indole- and benzodiazepine-binding region of human serum albumin. *Biochem. J.* **273**:641–644 (1991).
9. M. H. Rahman, K. Yamasaki, and Y. H. Shin. C.C. Lin, and M. Otagiri. Characterization of high affinity binding sites of nonsteroidal anti-inflammatory drugs with respect to site-specific probes on human serum albumin. *Biol. Pharm. Bull.* **16**:1169–1174 (1993).
10. S. Wanwimolruk, D. J. Birkett, and P. M. Brooks. Structural requirements for drug binding to site II on human serum albumin. *Mol. Pharmacol.* **24**:458–463 (1983).
11. M. Dockal, D. C. Carter, and F. Ruker. The three recombinant domains of human serum albumin. Structural characterization and ligand binding properties. *J. Biol. Chem.* **274**:29303–29310 (1999).
12. A. A. Spector. Fatty acid binding to plasma albumin. *J. Lipid. Res.* **16**:165–179 (1975).
13. S. Curry, P. Brick, and N. P. Franks. Fatty acid binding to human serum albumin: New insights from crystallographic studies. *Biochim. Biophys. Acta* **1441**:131–140 (1999).
14. J. A. Hamilton, D. P. Cistola, J. D. Morrisett, J. T. Sparrow, and D. M. Small. Interactions of myristic acid with bovine serum albumin: a ^{13}C NMR study. *Proc. Natl. Acad. Sci. USA* **81**:3718–3722 (1984).
15. J. A. Hamilton, S. Era, S. P. Bhamidipati, and R. G. Reed. Locations of the three primary binding sites for long-chain fatty acids on bovine serum albumin. *Proc. Natl. Acad. Sci. USA* **88**: 2051–2054 (1991).
16. G. Wilding, R. C. Feldhoff, and E. S. Vesell. Concentration-dependent effects of fatty acids on warfarin binding to albumin. *Biochem. Pharmacol.* **26**:1143–1146 (1977).
17. N. Rietbrock, G. Menke, G. Reuter, A. Lassmann, and R. Schmeidl. Influence of palmitate and oleate on the binding of warfarin to human serum albumin: stopped-flow studies. *J. Clin. Chem. Clin. Biochem.* **23**:719–723 (1985).
18. H. Vorum and B. Honore. Influence of fatty acids on the binding of warfarin and phenprocoumon to human serum albumin with relation to anticoagulant therapy. *J. Pharm. Pharmacol.* **48**:870–875 (1996).
19. I. Petitpas, A. A. Bhattacharya, S. Twine, M. East, and S. Curry. Crystal structure analysis of warfarin binding to human serum albumin: Anatomy of drug site I. *J. Biol. Chem.* **276**:22804–22809 (2001).
20. J. R. Brown and P. Shockley. In P. Jost and O. H. Griffith (eds.), *Serum Albumin: Structure and Characterization of Its Ligand Binding Sites. Lipid-Protein Interactions*, Vol. 1.Wiley, New York, 1982, pp. 25–68.
21. A. A. Bhattacharya, T. Grune, and S. Curry. Crystallographic analysis reveals common modes of binding of medium and long-chain fatty acids to human serum albumin. *J. Mol. Biol.* **303**:721–732 (2000).
22. N. Takamura, T. Maruyama, and M. Otagiri. Effects of uremic toxins and fatty acids on serum protein binding of furosemide: possible mechanism of the binding defect in uremia. *Clin. Chem.* **43**:2274–2280 (1997).
23. N. A. Brown, A. G. Wilson, and J. W. Bridges. Chain length dependency of fatty acid and carbamate binding to serum albumin. *Biochem. Pharmacol.* **31**:4019–4029 (1982).
24. U. Kragh-Hansen. Structure and ligand binding properties of human serum albumin. *Dan. Med. Bull.* **37**:57–84 (1990).